International Journal of Mass Spectrometry 304 (2011) 29–35

Contents lists available at ScienceDirect

International Journal of Mass Spectrometry

journal homepage: www.elsevier.com/locate/ijms

Photodissociation of indium oxide cluster cations

A.M. Knight, B. Bandyopadhyay, C.L. Anfuso, K.S. Molek, M.A. Duncan*

Department of Chemistry, University of Georgia, Athens, GA 30602-2556, United States

ARTICLE INFO

Article history:
Received 29 January 2011
Received in revised form 10 March 2011
Accepted 11 March 2011
Available online 17 March 2011

Keywords:
Metal oxide cluster ion
Photodissociation
Density functional theory

ABSTRACT

Indium oxide cations of the form $In_nO_m^+$ are produced by laser vaporization in a pulsed nozzle source and detected with time of flight mass spectrometry. The In_2O^+ and In_3O^+ ions have high relative intensities in the mass spectra of clusters sampled directly from the source. Cluster cations are mass-selected and photodissociated using the third harmonic (355 nm) of a Nd:YAG laser. The elimination of indium cation is the dominant loss channel for all cluster cations. However, certain other clusters, i.e., In_2O^+, In_2O_2, In_3O^+ and $In_3O_2^+$ are produced as fragments from several cluster sizes and are thus identified as particularly stable. Density functional theory calculations are employed for selected species to determine their structures and relative stabilities. The Wade–Mingos electron counting rules are found to be inappropriate for these systems because their bonding is primarily ionic.

1. Introduction

Metal oxide nanoparticles have applications in diverse areas of magnetic materials, catalysis, and medicine [1–7]. In this regard, main group metal systems are expected to have properties quite different from those of the transition metals. Whereas transition metal oxides are often employed in catalysis [2,3], main group metals such as indium often form semiconducting oxide nanoparticles, nanotubes or nanobelts [8–10], with applications in areas such as gas sensors [11–13]. Gas phase studies of metal oxide clusters provide finite-sized systems with which to investigate the details of structure and bonding systematically [14]. However, while there are many studies of transition metal oxides in the gas phase, there are few examples of corresponding main group systems [15–17]. In this study, we investigate the structure and bonding of small indium oxide cluster cations.

Transition metal oxide clusters in the gas phase have been found to have localized M–O–M–O bonding, although the oxidation states seen in the gas phase systems are not always the same as those in the bulk solids [18–20]. By contrast, the bonding in main group metal clusters and their alloys are often successfully described using the Wade–Mingos (WM) Rules, a simple model based on electron counting, which implies delocalized or multicentered bonding [21,22]. This model was originally developed to explain the stabilities of Zintl ions, which are well known in inorganic chemistry, and it can be used to predict stabilities of many kinds of electron deficient clusters. The clusters take on polyhedral structures to maximize the sharing of electron density in the interior of the cluster. This results in a system where closed shell species have n metal atoms and $2n+2$, $2n+4$, and $2n+6$ valence p electrons, which correspond to *closo*, *nido*, and *arachno* cluster forms, respectively. Gas phase analogues of the condensed phase Zintl ions have been studied for various main group metal alloy clusters that combine electron deficient metals with those having a relative excess of charge [23–25]. These systems have all successfully been described using the WM rules. There are only limited examples of main group metal oxides studied in the gas phase [15–17]. Unusual stoichiometries have been documented for these systems, but no general guiding principles have been derived to predict cluster stability.

Previous work on various metal oxide clusters has shown that it is difficult to gauge relative cluster stabilities on the basis of simple mass spectrometry [18–20]. Source and growth conditions can significantly affect the distribution of clusters observed. In mass spectrometric experiments, some form of ionization is always required. The detection efficiency using photoionization or electron impact ionization of metal clusters suffers from unknown ionization potentials, size-dependent cross sections, and fragmentation processes. Identification of particularly stable clusters from mass spectrometric intensity patterns is therefore not reliable. Our previous work has demonstrated that mass-selected photodissociation of metal compound cluster ions can be used successfully to determine which stoichiometries are more stable [20]. These stable clusters may or may not be prominent in the mass spectrum, but they are more likely to be resistant to decomposition and are produced more frequently than other species during the fragmentation of larger clusters. In addition to the transition metal oxides, these methods have been applied

* Corresponding author. Tel.: +1 706 542 1998; fax: +1 706 542 1234.
E-mail address: maduncan@uga.edu (M.A. Duncan).

1387-3806/$ – see front matter © 2011 Elsevier B.V. All rights reserved.
doi:10.1016/j.ijms.2011.03.005

to study various metal carbides [26] and metal silicon clusters [27].

Previous studies have investigated the mass spectrometry of pure indium clusters in the gas phase [28–33]. The pure indium cluster In_{11}^{7-} was also produced via condensed-phase chemistry, and found to follow the WM electron counting rules [34,35]. Mixed metal alloys of indium have been studied in the gas phase and also found to follow the predictions of the WM rules [24]. In the only study of indium oxides, Janssens et al. investigated the monoxide clusters with mass spectrometry and theoretical calculations [17]. These workers found that the In_3O^+ cation and the In_7O neutral cluster were more stable than others studied. In the present paper, we produce and study more heavily oxidized indium clusters, using mass spectrometry and mass-selected photodissociation measurements. The prominent clusters in these fragmentation studies are then evaluated in the context of WM rules and studied using density functional theory computations to investigate their structure and bonding.

2. Experimental

Metal oxide cations are produced by laser vaporization using a pulsed nozzle cluster source. The third harmonic (355 nm) of an Nd:YAG laser (Spectra Physics GCR-11) is used to vaporize metal from the surface of a rotating and translating indium rod. Helium gas seeded with either O_2 or N_2O, at a concentration of 1–5%, is pulsed over the rod with a General Valve (Series 9; 60 psi backing pressure, 1 mm orifice). The sample holder has a 5 mm bore diameter and a 1.0 in. long growth channel to encourage cluster growth. The cluster cations grow directly in the laser plasma and are skimmed into the mass spectrometer as a molecular beam. Clusters are mass-analyzed and size-selected for photodissociation experiments using a specially designed reflectron time-of-flight (RTOF) mass spectrometer [36]. A pulsed acceleration field extracts the clusters from the molecular beam into the RTOF instrument. For the photodissociation studies, pulsed deflection plates in the first section of the flight tube allow for mass selection of the desired cluster. Selected ions are then excited in the turning region of the reflectron with a second Nd:YAG laser operating at either 532 nm or 355 nm (Spectra Physics DCR-3). The parent ions and any fragments produced from the photoexcitation process are mass analyzed in the second leg of the reflectron and subsequently detected by an electron multiplier tube and digital oscilloscope (LeCroy 9310A). The data are transferred from the oscilloscope to a computer using an IEEE-488 interface. Studies were performed as a function of photodissociation laser power, which ranged from 10 to 60 mJ/cm^2-pulse (unfocused).

The photodissociation spectra are generated using a computer difference method, where the intensity of the parent ion signal with no photodissociation laser present is subtracted from the parent + fragment signals measured when this laser is on. This gives a negative parent ion peak indicating its photo-depletion and positive-going fragment ion peaks. Ideally, the integrated peak intensities would equal the amount of depletion. However, mass discrimination effects make it difficult to focus equally on parent and fragment ions [36]. Therefore, we cannot give any quantitative branching ratios and simply distinguish between strong and weak fragment channels.

Density functional theory computations were carried out using the Gaussian 03W program package [37] to investigate structures for the most prevalent cations and neutrals in these studies, using the B3LYP (Becke-3-Lee–Yang–Parr) functional [38–39]. The basis sets used were the 6-311+G* for oxygen and the LANL2DZ for indium atoms [40].

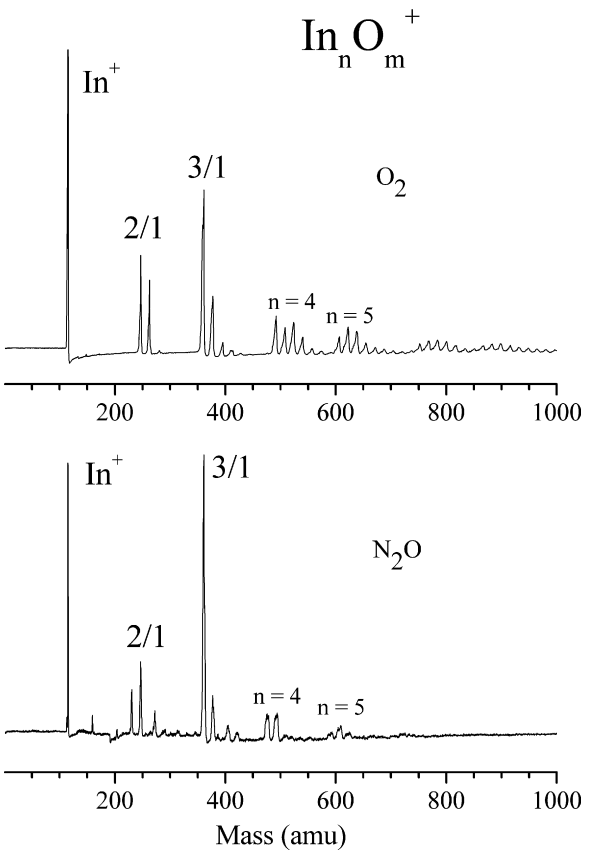

Fig. 1. Time-of-flight mass spectrum for $In_nO_m^+$ clusters formed in a helium expansion seeded with either O_2 (upper trace) or N_2O (lower trace).

3. Results and discussion

The mass spectra of $In_nO_m^+$ cluster cations are shown in Fig. 1. Clusters produced using an He/O_2 expansion are shown in the top pane, and those produced using a He/N_2O expansion are shown in the lower pane. Though some of the larger clusters seen in the He/O_2 expansion are not found with N_2O, the cluster distribution is essentially the same with both gas mixtures. Cations up to the range of $n = 6$ are observed, with the metal ion, In^+, and the species In_2O^+ and In_3O^+ prominent in both spectra. These and subsequent cation stoichiometries are designated as $1/0^+$, $2/1^+$, and $3/1^+$ in the following discussion. It is interesting to note that the $4/0^+$ and $4/1^+$ species are not observed in the He/N_2O expansion. The first clusters seen for the $n = 4$ and $n = 5$ groups are the $m = 2$ species (i.e., $4/2^+$ and $5/2^+$). Likewise, except for the strong atomic ion signal, there are essentially no pure indium clusters present. Cluster production for $n \geq 5$ varies greatly with source conditions, and no prominent ions are detected in this higher mass range.

Mass-selected photofragmentation experiments are performed to investigate the relative stabilities of selected clusters. Individual cluster cations with sufficient intensity are mass selected and then photodissociated by laser excitation at 355 nm. Photodissociation experiments are also attempted with 532 nm light, but fragmentation at this wavelength is not nearly as efficient as with 355 nm for any cluster. The 532 nm photon energy may be too low to cause efficient fragmentation, or the absorption cross section at this wavelength may be too small. In the limited data available at this wavelength, the dissociation channels were the same as those seen for 355 nm. In studies of the laser fluence dependence, fragmentation was observed for fluences as low as 10 mJ/cm^2 at 355 nm; most of the clusters fragment efficiently with 30 mJ/cm^2. The

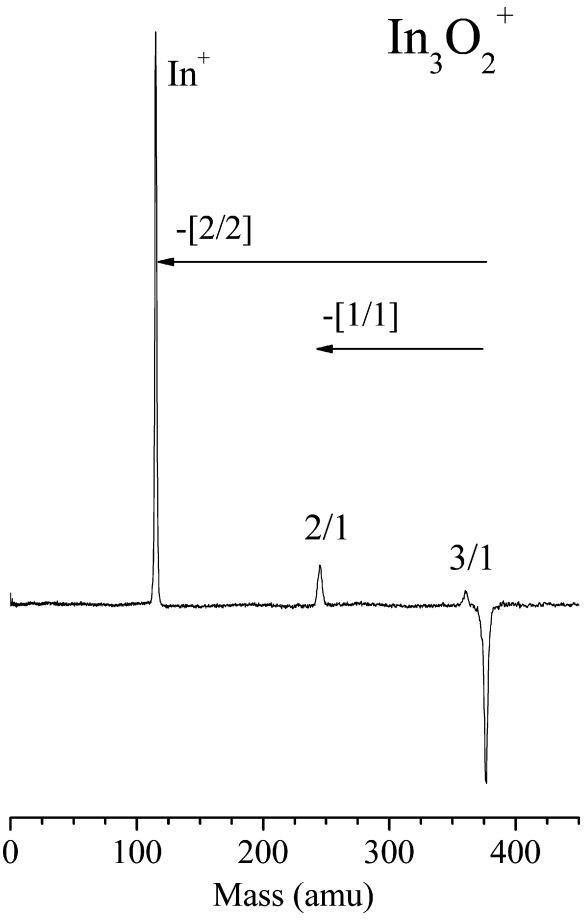

Fig. 2. Photodissociation mass spectrum of $In_3O_2^+$ at 355 nm with apparent neutral losses indicated.

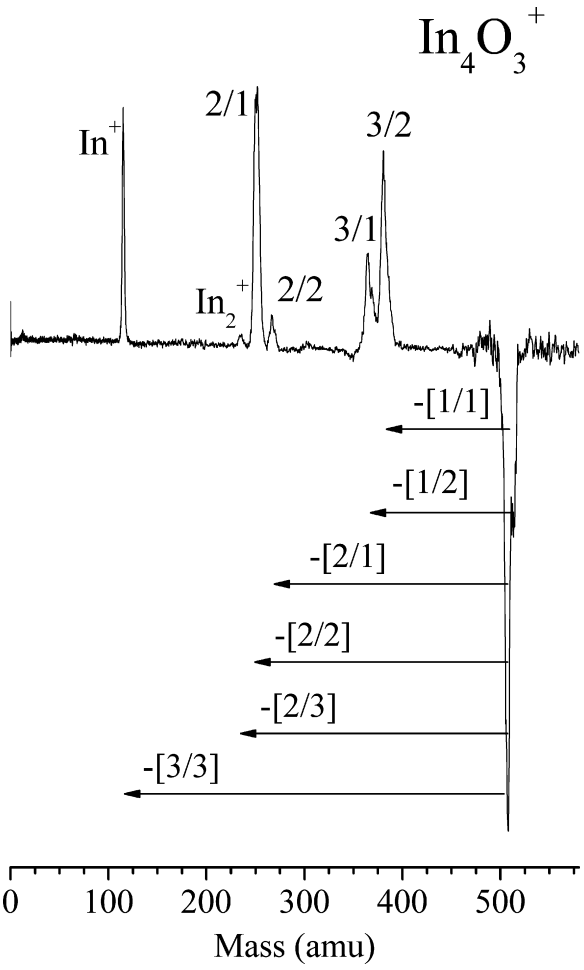

Fig. 3. Photodissociation mass spectrum of $In_4O_3^+$ at 355 nm with apparent neutral losses indicated.

interpretation of these photodissociation experiments has been discussed extensively in our previous papers [20,26,27]. While no single fragmentation spectrum necessarily offers reliable insight, the prominent cation clusters produced repeatedly as photofragments become evident when several clusters are studied. Likewise, similar patterns may be seen in the common neutrals lost. We present selected examples of the photodissociation mass spectra in Figs. 2–4, and a complete list of fragmentation channels for each cluster cation studied is provided in Table 1.

In the photodissociation data, as in the mass spectra, the metal cation and the $2/1^+$ and $3/1^+$ clusters are quite prominent. Their appearance in all the photodissociation spectra indicate that these latter molecular ion species are relatively more stable than other cluster stoichiometries. In addition to these, $3/2^+$ is prominent in the photodissociation data for the $n > 3$ parent clusters which are large enough to produce it. Also, the $4/3^+$ fragment is a small but convincing product in the photodissociation of the $5/3^+$ parent cation. However, the $4/3^+$ fragment does not appear in the photodissociation of the larger $5/4^+$ or $5/5^+$ cations.

Neutral photofragments are not detected directly in these experiments, but are inferred by mass conservation. For example, in the photodissociation of the $3/2^+$ cluster (Fig. 2), the atomic ion product could be formed by the loss of the 2/2 neutral cluster, or from the sequential loss of two smaller clusters (i.e., 2/1 and 0/1, 1/1 and 1/1, or 1/0 and 1/2). We cannot distinguish between these alternatives, and thus the neutral loss channels throughout this study are placed in brackets (e.g., [2/2]) to indicate this uncertainty. In general, the elimination of larger molecular products is lower in energy than the elimination of smaller molecules or atoms because of the additional bonds that must be broken. For this discussion, therefore, we will treat the fragmentation as if it is the loss of a single neutral cluster, but this in no way implies certainty on this point.

Table 1
The stoichiometries of indium oxide photofragments ($In_nO_m^+ = n,m$) detected using 355 and 532 nm. Most prevalent photofragments in bold. Neutral losses below ([n/m]).

Parent cation cluster	Photofragments
3/1	**2/1**; 2/0; **1/0**, 0/1 [1/0];[1/1];[2/1];[3/0]
3/2	**3/1**; **2/1**; **1/0** [0/1];[1/1];[2/2]
3/3	**2/1**; **1/0**; 0/1 [1/2];[2/3];[3/2]
4/2	**3/1**; **2/1**; 2/0; **1/0** [1/1];[2/1];[2/2];[3/2]
4/3	**3/2**; **3/1**; 2/2; **2/1**; 2/0; **1/0** [1/1];[1/2];[2/1];[2/2];[2/3];[3/3]
4/4	4/2; **3/2**; **3/1**; **2/1**; 1/1; **1/0** [0/2];[1/2];[1/3];[2/3];[3/3];[3/4]
5/2	**3/2**; **3/1**; **2/1**; **1/0**; 0/1 [2/0];[2/1];[3/1];[4/2];[5/1]
5/3	**3/2**; **3/1**; **2/1**; **1/0**; 0/1 [2/1];[2/2];[3/2];[4/3];[5/2]
5/4	4/3; **3/2**; **3/1**; **2/1**; **1/0**; 0/1 [1/1];[2/2];[2/3];[3/3];[4/4][5/3]
5/5	5/4; 5/3; **3/2**; **3/1**; **2/1**; **1/0**; 0/1 [0/1];[0/2];[2/3];[2/4];[3/4];[4/5];[5/4]

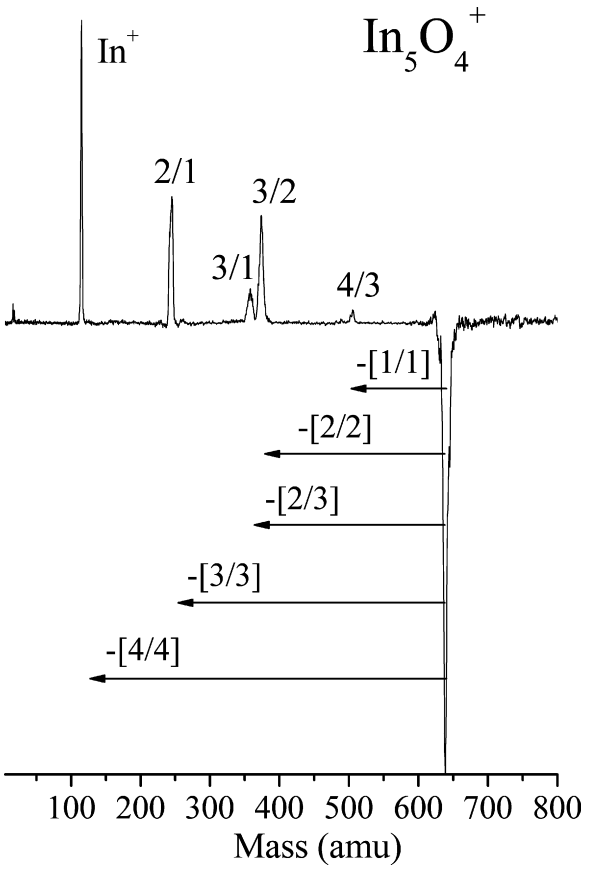

Fig. 4. Photodissociation mass spectrum of $In_5O_4^+$ at 355 nm with apparent neutral losses indicated.

The most prominent feature of the photodissociation data is the ubiquitous appearance of the In^+ fragment. This is at first surprising because the ionization potentials (IPs) of metal atoms are usually higher than those of its clusters [41]. Photodissociation usually produces charged species that have lower ionization potentials because this is a lower energy process. However, indium is somewhat unusual in this regard, having an atomic ionization potential (5.79 eV) that is quite low, even lower than those of its small clusters [28a]. In general, metal oxides have higher ionization potentials than pure metals [42]. In the case of the present In_nO_m species, not all relevant IPs are known, but selected species were studied by Jannsens et al. using photoionization spectroscopy [17]. The IPs determined for the 2/1 and 3/1 clusters were >6.43 and 5.08 eV, respectively. The computational work in the Jannsens study determined the IP of InO and In_2O to be 8.9 and 7.5 eV [17], and our computational work (see below) finds a value of 8.1 eV for the 2/2 species. Given these known or approximate energetics, it is possible to explain the prevalence for the loss of the metal ion, and some of the other dissociation channels seen. In the case of the $In_3O_2^+$ dissociation (Fig. 2), the main channel of $3/2^+ \rightarrow In^+ + [2/2]$ is then understandable because the IP of In is less than that of 2/2. Likewise the minor channel of $3/2^+ \rightarrow 2/1^+ + [1/1]$ makes sense because the IP of 2/1 is less than that of 1/1. Similar reasoning explains some of the channels in the dissociation of $In_4O_3^+$ in Fig. 3, such as $4/3^+ \rightarrow 2/1^+ + [2/2]$. As cluster size grows, and more different fragment ions are involved, we do not know enough of the required energetics to make such conclusions. However, the behavior in the smaller clusters is completely consistent with the charge occurring on the lower IP fragment, and therefore it is safe to assume that this is also the case for the larger systems.

Related to this, other than in the case of the $3/1^+$ ion producing the $2/1^+$ fragment, we do not see any of the charged intermediates that would correspond to the loss of neutral indium. Specifically, we do not see $2/2^+$, $3/3^+$, etc. However, we do see evidence for the neutral intermediates, i.e., [2/2], [3/3], [4/4], etc. which would be expected for the loss of In^+ from $3/2^+$, $4/2^+$, $4/3^+$, $5/3^+$ and $5/4^+$. This is all consistent with the In^+ being eliminated directly in these photodissociation processes, leaving behind the corresponding neutral $In_{n-1}O_m$. There have been other examples where the metal cation was seen as a photofragmentation product rather than larger cluster ions, as in the case of titanium carbides [26]. Rayane et al. also observed that the metal cation loss channel was the dominant process for fragmentation in pure indium clusters, which they rationalized in terms of the atom's relatively low IP compared to larger pure indium clusters [28a].

There is also an interesting pattern in the stoichiometries of the inferred neutral fragments. Again assuming that these are eliminated as a single cluster, the photodissociation data (Table 1) show evidence for the loss of [1/1], [2/2], [3/3] and [4/4], respectively in almost every photodissociation sequence. [2/2] is particularly noticeable, for example, in the main photofragments in Figs. 2–4. The 1:1 stoichiometry of InO is different from that of bulk indium oxide, which is In_2O_3 [43]. The oxidation state of +2 suggested for the indium here has been observed before, but compounds based on this are highly reactive [43]. The observation of different oxidation states for gas phase clusters compared to the bulk material has been noted before in the photodissociation of several transition metal oxides [20]. For example, the most stable phase of iron oxide has the same M_2O_3 bulk stoichiometry as indium oxide, but the less stable FeO stoichiometry was observed exclusively throughout the growth and photodissociation of the gas phase clusters [20d]; the 2/3 stoichiometry was not seen at all in the photodissociation channels. However, the [2/3] loss is seen occasionally here (Table 1), but it occurs only as a minor channel in the photodissociation of the $3/3^+$, $4/3^+$, $4/4^+$, $5/4^+$and $5/5^+$ cations.

Not only is the neutral 2/3 indium oxide stoichiometry not prominent here, there is also little evidence for other cation clusters having the normal +3 oxidation state of In. Cations such as InO^+ or $In_3O_4^+$, all having the general formula of $InO^+(In_2O_3)_n$, would be expected, but none of these are found. This observation is surprising because the corresponding $AlO^+(Al_2O_3)_n$ stoichiometries dominated the mass spectrum of aluminum oxide clusters that were studied previously [16].

It is interesting to consider what insight may be gained into the stability of certain clusters by the application of the WM rules of electron counting. This model describes clusters that are electron deficient and form polyhedral structures in order to share electron density. Previous studies by our group and others on main group alloy clusters (e.g., Sn/Bi, Pb/Sb) [23–25] demonstrated that certain clusters formed in high abundance were consistent with the predictions of these rules. While the bonding in these main group metal alloy clusters seems to follow the predictions of electron counting, it is not clear that this will also be true for their oxides, which tend to form stronger bonds. While the main group elements in the second row (boron, carbon) employ *s*–*p* hybridization in their bonding, the valence *s* and *p* orbitals are more separated in energy for the heavier elements, the *s* orbitals are more "inert", and hybridization is progressively less likely [43]. Therefore, only the valence *p* electrons are considered for electron counting. We then count one *p* electron for each indium atom and four for each oxygen atom, and evaluate the electron count for each cluster value up to $n = 10$, where n is the total number of cluster atoms. The resulting electron counts are shown in Table 2. Of the species predicted to be stable, we observe [2/2], [2/3] and [4/4] in the fragmentation experiments. The $5/4^+$ and $5/5^+$ ions are seen in the mass spectra, but not detected as photofragments, perhaps because larger clusters could not be

Table 2
Wade's Rules electron counts and structural assignments for selected indium oxide stoichiometries.

Cluster	p electron count	Wade's Rule structural assignment
In_2O^+	5	–
In_2O	6	–
In_2O_2	10	*Closo*
In_2O_3	14	*Nido*
In_3O^+	6	–
$In_3O_2^+$	10	–
$In_3O_3^+$	14	*Closo*
In_3O_3	15	–
$In_4O_2^+$	11	–
$In_4O_3^+$	15	–
$In_4O_4^+$	19	–
In_4O_4	20	*Nido*
$In_5O_2^+$	12	–
$In_5O_3^+$	16	–
$In_5O_4^+$	20	*Closo*
$In_5O_5^+$	24	*Nido*

studied with photodissociation. While some of the predicted stoichiometries are apparently observed for inferred neutrals, the most prominent ions detected here do not follow the WM rules. Apparently, electron counting is not a sufficient model for the bonding in these oxide cations. As stated previously, this is not surprising given the strong covalent and ionic nature of the metal oxide bonding. Since electron counting is based on $2n+2$, $2n+4$, and $2n+6$, it is not surprising that it is not successful for clusters with an odd number of electrons, such as In_2O^+ or In_3O_3. The application of the WM rules also is based on delocalized bonding, and it is not clear that this picture is appropriate for these systems.

To investigate cluster structures and the detailed nature of the bonding (ionic versus covalent, localized versus delocalized), we employ DFT calculations on several of the prominent clusters seen here. Selected examples of the structures obtained in these calculations are shown in Fig. 5 and the full list of calculated energetics is given in Table 3. The $2/1^+$ cluster is predicted to be a doublet with a linear structure. Calculations on the 2/2 neutral cluster investigated both singlet and triplet spin states, finding that the singlet state is lower in energy, but the two structures were qualitatively similar. Both are linear with alternating oxygen and indium atoms. The $2/2^+$ cation has a similar linear structure. Rectangular structures for the 2/2 neutral and cation lie slightly higher in energy than the linear species. The $3/1^+$ cluster has a singlet ground state; the calculation for the triplet state of this cation did not converge. In previous theoretical work, Janssens et al. [17] found this cation to have a planar D_{3h} structure. Its bonding was discussed in terms of a resonance hybrid of three In-O covalent bonds and three ionic bonds ($3\ In^+ + O^{2-}$). As shown in Fig. 5, calculations here find this same structure, which has the oxygen atom interacting with three metal atoms. The 2/3 and 3/2 clusters both have different structures for the neutrals and cations. The $3/2^+$ cation is a linear singlet, with alternating metal and oxygen atoms; its structure is shown in Fig. 5. The 2/3 neutral is also a linear singlet with the inverse of the $3/2^+$ cation structure. The neutral 3/2 and $2/3^+$ both have cyclic doublet structures, like that shown for the 3/2 species in Fig. 5; again, the $2/3^+$ has the inverse of the 3/2 structure. The 4/3 neutral and cation have the same structure, with a ring inserted in the middle of an otherwise linear species; the $4/3^+$ structure is shown in Fig. 5.

As can be seen in Fig. 5 and Table 3, essentially all of the lowest energy structures obtained involve alternating oxygen and indium atoms in linear structures. There are few terminal oxygens in these structures, which are prominent in many transition metal oxides [18–20], and there are no indium–indium bonds. The exception to linear structures in the small clusters is the $3/1^+$ species, which has a central oxygen with indium atoms situated like the spokes of a wheel. Its structure highlights the instability of indium–indium

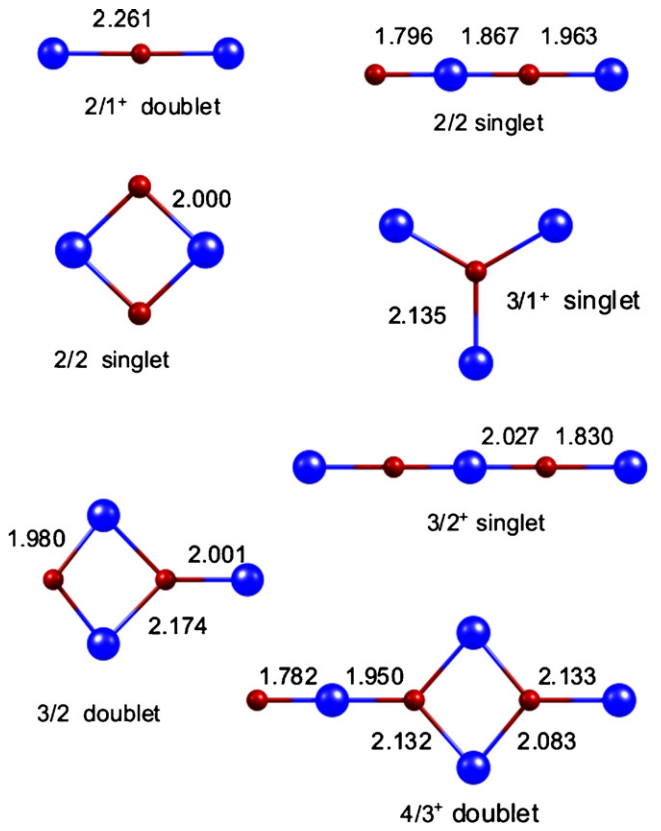

Fig. 5. Structures from DFT calculations for selected indium oxide neutral and cationic clusters.

Table 3
Energetics calculated for indium oxide neutral and cationic clusters using DFT.

Cluster	Energy (HF)	Rel. energy (kcal/mol)	Energy/bond (kcal/mol)
$2/1^+$ (doublet)	−78.7839103	0.0	65.5
2/2 (singlet, linear) O–In–O–In	−154.2947846	0.0	87.6
2/2 (singlet, cyclic)	−154.2768676	+11.24	62.9
2/2 (triplet, cyclic)	−154.2617515	+20.73	60.5
2/2 (triplet, linear) O–In–In–O	−154.1924401	+64.23	66.2
$2/2^+$ (doublet, linear) O–In–O–In	−153.9913657	0.0	68.2
$2/2^+$ (doublet, cyclic)	−153.9494454	+26.31	44.6
$2/2^+$ (doublet, linear) O–In–In–O	−153.8588092	+83.2	40.5
2/3 (singlet, linear)	−229.4731609	0.0	79.6
2/3 (singlet, cyclic)	−229.4354712	+23.65	58.9
2/3+ (doublet, linear)	Unstable		
2/3+ (doublet, cyclic)	−229.1602922	0.0	50.9
$3/1^+$ (singlet, cyclic)	−80.8063328	0.0	80.1
$3/1^+$ (singlet, linear)	−80.7742528	+20.13	73.4
3/2 (doublet, linear)	Unstable		
3/2 (doublet, cyclic) In on end	−156.2612138	0.0	67.4
3/2 (doublet, cyclic) O on end	−156.1726022	+55.61	70.3
$3/2^+$ (singlet, linear) In–O–In–O–In	−156.0566867	0.0	85.2
$3/2^+$ (triplet, cyclic)	−155.9987834	+36.34	60.9
$3/2^+$ (singlet, cyclic)	−155.9680558	+55.62	71.3
$3/2^+$ (triplet, linear) In–O–In–O–In	−155.9328739	+77.70	65.8
4/3 (singlet, ring)	−233.4305668	0.0	68.7
$4/3^+$ (doublet, ring)	−233.1732277	0.0	64.7

bonding, which would be required if this species adopted a linear structure. Interestingly, this multiply connected oxygen in the rectangular theme closely resembles the structure of the [0 0 1] surface of indium oxide nanobelts [9]. Only at the largest cluster size studied (4/3) do structures containing rings become more stable. The vertices of these rings again have the three-centered oxygen bonding motif. There are clearly no three-dimensional structures in these small clusters. This would be required for efficient spatial overlap of metal *p* orbitals in the center volume of the cluster, which is a common feature of delocalized bonding in main group metal alloy clusters [21–25]. The lack of any apparent applicability of the WM electron counting rules to these systems therefore is completely understandable. The importance of linear structures with alternating atoms is consistent with a strong ionic component in the bonding, which makes sense because of the large difference between the ionization potentials of indium and oxygen. However, it is still interesting that the structures, stoichiometries and effective oxidation states found here are significantly different from those of aluminum oxide clusters, which also have a strong ionic component in their bonding. Aluminum oxide clusters in the small size range do not take on linear structures, but rather prefer 2-dimensional and even 3-dimensional structures [44].

Our computational data also makes it possible to compare the relative stability of these various ions and neutrals. We do this systematically by comparing the energy of each cluster to that of its separated atoms. To make this comparison as fair as possible, this condensation energy is then normalized to the number of bonds present, allowing a per-bond stability to be obtained for each cluster. These data are also presented in Table 3. As shown, DFT computations indicate per-bond energies in the 40–90 kcal/mol range; all of the stable ground state structures have per-bond energies of 65 kcal/mol or greater. The highest per-bond energies occur for 2/2, $3/1^+$ and $3/2^+$, which are all prominent photofragments for multiple parent ions. The only prominent photofragment without a high per-bond energy is the $2/1^+$ cation. The only cluster with a high per-bond stability that is not also prominent as a photofragment is the neutral 2/3 species, which has the bulk stoichiometry. It is somewhat evident as a neutral leaving group in the larger clusters here, and would perhaps become more prominent if larger clusters could be produced and studied. Therefore, the per-bond energies seem to confirm at least some of the conclusions of the photodissociation data.

The structures and stabilities of these clusters provide additional insight into the dissociation channels and dynamics. For example, because of the linear structures of $3/2^+$ and 2/2, the fragmentation $3/2^+ \rightarrow In^+ + [2/2]$ can be viewed as the breaking of a single bond in a linear chain. In the dissociation of the $4/3^+$ ion, the most abundant photofragment is the $2/1^+$ ion. $2/1^+$ is itself apparently stable, but it is accompanied by the loss of the stable [2/2] neutral. This channel therefore has favorable energetics from both of the fragments. It is tempting to imagine the cleavage of two opposite bonds in the ring area of the $4/3^+$ structure to accomplish this efficiently. The process $5/4^+ \rightarrow 3/2^+ + [2/2]$ has a similarly favorable combination of ionic and neutral fragments, as do most of the other prominent fragmentation channels seen. The exceptions to this trend involve the production of $3/1^+$ as a photofragment. Although it is extremely abundant in the clusters that grow in the source, and is computed to have one of the highest per-bond stabilities, this ion is not the most abundant fragment from any of the dissociation processes studied. This is understandable in light of the unique structure of this ion and its corresponding neutral co-fragments. Generating $3/1^+$ from virtually any of the ground state parent ions studied here requires the breaking of 2–3 bonds and significant rearrangement of atoms. Moreover, the co-fragments resulting (i.e., $3/2^+ \rightarrow 3/1^+ + O$; $4/3^+ \rightarrow 3/1^+ + [1/2]$) are not particularly stable neutrals. Considering this, the fact that $3/1^+$ is seen at all as a fragment attests to its high stability, consistent with its prominence in the initial cluster growth and its computed thermochemistry.

4. Conclusions

Small indium oxide clusters produced by laser vaporization have been investigated with time-of-flight mass spectrometry and mass-selected photodissociation. We observe a distribution of cluster stoichiometries, but the In_3O^+ ion is remarkably abundant under all source conditions. Photodissociation of prominent clusters identifies the main fragmentation products as the indium atomic cation, and the In_2O^+, $In_3O_2{}^+$ and In_3O^+ molecular ions. Many of the clusters lost neutrals of the form $(InO)_n$; of these the In_2O_2 occurred frequently and was computed to be quite stable. The $In_4O_3{}^+$ ion and the In_2O_3 neutral are also suggested by theory to have similar high stability, but these are not as prominent as photofragments, possibly because the clusters studied were relatively small. Trends throughout the data suggest that indium tends toward an oxidation state of +2 rather than +3 in these clusters. Although the Wade–Mingos rules can be "forced" to fit the numerology of some clusters, this model does not appear to be appropriate for these systems because their bonding is primarily ionic in character. However, the ionic bonding here results in very different stoichiometries and structures than those seen for the corresponding aluminum oxide clusters.

Acknowledgement

We gratefully acknowledge generous support for this work from the Air Force Office of Scientific Research (Grant No. FA95509-1-0166).

References

[1] K.J. Klabunde, Nanoscale Materials in Chemistry, Wiley Interscience, New York, 2001.
[2] D.L. Feldheim, C.A. Foss (Eds.), Metal Nanoparticles, Marcel Dekker, New York, 2002.
[3] G.A. Ozin, A.C. Arsenault, Nanochemistry, Royal Society of Chemistry Publishing, Cambridge, U.K., 2005.
[4] M.T. Pope, A. Müller, Poloyoxometalate Chemistry From Topology via Self-Assembly to Applications, Kluwer, Boston, 2001.
[5] D.C. Crans, J.J. Smee, E. Gaidamauskas, L.Q. Yang, Chem. Rev. 104 (2004) 849.
[6] M. Fernandez-Garcia, A. Martinez-Arias, J.C. Hanson, J.A. Rodriguez, Chem. Rev. 104 (2004) 4063.
[7] Y. Gong, M. Zhou, Chem. Rev. 109 (2009) 6765.
[8] Z.W. Pan, Z.R. Dai, Z.L. Wang, Science 291 (2001) 1947.
[9] X.Y. Kong, Z.L. Wang, Solid State Commun. 128 (2003) 1.
[10] Y. Liu, W. Yang, D. Hou, Superlattices Microstruct. 43 (2008) 93.
[11] D. Zhang, C. Li, X. Liu, S. Han, T. Tang, C. Zhou, Appl. Phys. Lett. 83 (2003) 1845.
[12] Q. Wan, E.N. Dattolo, W.Y. Fung, W. Guo, Y. Chen, X. Pan, W. Lu, Nano Lett. 6 (2006) 2909.
[13] A. Gurlo, Angew. Chem. Int. Ed. 49 (2010) 5610.
[14] H. Haberland, Clusters of Atoms and Molecules, vols. I and II, Springer Series in Chemical Physics, Springer-Verlag, New York, 1995.
[15] M.R. France, J.W. Buchanan, J.C. Robinson, S.H. Pullins, J.L. Tucker, R.B. King, M.A. Duncan, J. Phys. Chem. 101 (1997) 6214.
[16] D. van Heijnsbergen, K. Demyk, M.A. Duncan, G. Meijer, G. von Helden, Phys. Chem. Chem. Phys. 5 (2003) 2515.
[17] E. Janssens, S. Neukermans, F. Vanhoutte, R.E. Silverans, P. Lievens, A. Navarro-Vásquez, P.V.R. Schleyer, J. Chem. Phys. 118 (2003) 5862.
[18] (a) R.C. Bell, K.A. Zemski, K.P. Kerns, H.T. Deng, A.W. Castleman Jr., Phys. Chem. A 102 (1998) 1733;
(b) R.C. Bell, K.A. Zemski, D.R. Justes, A.W. Castleman Jr., J. Chem. Phys. 114 (2001) 798;
(c) K.A. Zemski, D.R. Justes, A.W. Castleman Jr., J. Phys. Chem. B 106 (2002) 6136.
[19] (a) M. Foltin, G.J. Stueber, E.R. Bernstein, J. Chem. Phys. 111 (1999) 9577;
(b) M. Foltin, G.J. Stueber, E.R. Bernstein, J. Chem. Phys. 114 (2001) 8971;
(c) Y. Matsuda, E.R. Bernstein, J. Phys. Chem. A 109 (2005) 314;
(d) F. Dong, S. Heinbuch, S.G. He, Y. Xie, J.J. Rocca, E.R. Bernstein, J. Chem. Phys. 125 (2006) 8.
[20] (a) K.S. Molek, T.D. Jaeger, M.A. Duncan, J. Chem. Phys. 123 (2005) 144313;
(b) K.S. Molek, Z.D. Reed, A.M. Ricks, M.A. Duncan, J. Phys. Chem. A 111 (2007) 8080;

(c) Z.D. Reed, M.A. Duncan, J. Phys. Chem. A 112 (2008) 5354;
(d) K.S. Molek, C. Anfuso-Cleary, M.A. Duncan, J. Phys. Chem. A 112 (2008) 9238.
[21] (a) K. Wade, J. Chem. Soc. D 10 (1971) 210;
(b) K. Wade, Adv. Inorg. Chem. Radiochem. 18 (1976) 1.
[22] (a) D.M.P. Mingos, Nat. Phys. Sci. 99 (1972) 236;
(b) D.M.P. Mingos, Acc. Chem. Res. 17 (1984) 311.
[23] (a) R.G. Wheeler, K. LaiHing, W.L. Wilson, J.D. Allen, R.B. King, M.A. Duncan, J. Am. Chem. Soc. 108 (1986) 8101;
(b) R.G. Wheeler, K. LaiHing, W.L. Wilson, M.A. Duncan, J. Chem. Phys. 88 (1988) 2831;
(c) K.F. Willey, K. LaiHing, T.G. Taylor, M.A. Duncan, J. Phys. Chem. 97 (1993) 7435.
[24] M.B. Bishop, K. LaiHing, P.Y. Cheng, M. Peschke, M.A. Duncan, J. Phys. Chem. 93 (1989) 1566.
[25] (a) R.W. Farley, A.W. Castleman Jr., J. Am. Chem. Soc. 111 (1989) 2734;
(b) R.W. Farley, A.W. Castleman Jr., J. Chem. Phys. 92 (1990) 1790;
(c) Y. Yamada, A.W. Castleman Jr., J. Chem. Phys. 97 (1992) 4543;
(d) U. Gupta, A.C. Reber, P.A. Clayborne, J.J. Melko, S.N. Khanna, A.W. Castleman Jr., Inorg. Chem. 47 (2008) 10953.
[26] (a) J.S. Pilgrim, M.A. Duncan, J. Am. Chem. Soc. 115 (1993) 4395;
(b) J.S. Pilgrim, M.A. Duncan, J. Am. Chem. Soc. 115 (1993) 9724;
(c) J.S. Pilgrim, M.A. Duncan, Int. J. Mass Spectrom. Ion Process. 138 (1994) 283;
(d) J.S. Pilgrim, L.R. Brock, M.A. Duncan, J. Phys. Chem. 99 (1995) 544;
(e) M.A. Duncan, J. Cluster Sci. 8 (1997) 239.
[27] J.B. Jaeger, T.D. Jaeger, M.A. Duncan, J. Phys. Chem. A 110 (2006) 9310.
[28] (a) D. Rayane, P. Melinon, B. Cabaud, A. Hoareau, B. Tribollet, M. Broyer, J. Chem. Phys. 90 (1989) 3295;
(b) B. Baguenard, M. Pellarin, C. Bordas, J. Lermé, J.L. Vialle, M. Broyer, Chem. Phys. Lett. 205 (1993) 13;
(c) E. Cottancin, M. Pellarin, J. Lermé, B. Palpant, B. Baguenard, J.-L. Vialle, M. Broyer, Z. Phys. D 40 (1997) 288.
[29] F.L. King, M.M. Ross, Chem. Phys. Lett. 164 (1989) 131.
[30] K.E. Schriver, J.L. Persson, E.C. Honea, R.L. Whetten, Phys. Rev. Lett. 64 (1990) 2539.
[31] (a) Z. Ma, S.R. Coon, W.F. Calaway, M.J. Pellin, D.M. Gruen, E.I. von Nagy-Felsobuki, J. Vac. Sci. Technol. A 12 (1994) 2425;
(b) A. Wucher, Z. Ma, W.F. Calaway, M.J. Pellin, Surf. Sci. 304 (1994) L439.
[32] J. Lermé, P. Dugourd, R.R. Hudgins, M.F. Jarrold, Chem. Phys. Lett. 304 (1999) 19.
[33] C. Staudt, A. Wucher, S. Neukermans, E. Janssens, F. Vanhoutte, E. Vandeweert, R.E. Silverans, P. Lievens, Nucl. Instrum. Methods Phys. Res. B 193 (2002) 787.
[34] S.C. Sevov, J.D. Corbett, Inorg. Chem. 30 (1991) 4875.
[35] R.B. King, I. Silaghi-Dumitrescu, Dalton Trans. (2008) 6083.
[36] D.S. Cornett, M. Peschke, K. LaiHing, P.Y. Cheng, K.F. Willey, M.A. Duncan, Rev. Sci. Instrum. 63 (1992) 2177.
[37] M.J. Frisch, G.W. Trucks, H.B. Schlegel, G.E. Scuseria, M.A. Robb, J.R. Cheeseman, J.A. Montgomery, Jr., T. Vreven, K.N. Kudin, J.C. Burant, J.M. Millam, S.S. Iyengar, J. Tomasi, V. Barone, B. Mennucci, M. Cossi, G. Scalmani, N. Rega, G.A. Petersson, H. Nakatsuji, M. Hada, M. Ehara, K. Toyota, R. Fukuda, J. Hasegawa, M. Ishida, T. Nakajima, Y. Honda, O. Kitao, H. Nakai, M. Klene, X. Li, J.E. Knox, H.P. Hratchian, J.B. Cross, C. Adamo, J. Jaramillo, R. Gomperts, R.E. Stratmann, O. Yazyev, A.J. Austin, R. Cammi, C. Pomelli, J.W. Ochterski, P.Y. Ayala, K. Morokuma, G.A. Voth, P. Salvador, J.J. Dannenberg, V.G. Zakrzewski, S. Dapprich, A.D. Daniels, M.C. Strain, O. Farkas, D.K. Malick, A.D. Rabuck, K. Raghavachari, J.B. Foresman, J.V. Ortiz, Q. Cui, A.G. Baboul, S. Clifford, J. Cioslowski, B.B. Stefanov, G. Liu, A. Liashenko, P. Piskorz, I. Komaromi, R.L. Martin, D.J. Fox, T. Keith, M.A. Al-Laham, C.Y. Peng, A. Nanayakkara, M. Challacombe, P.M. W. Gill, B. Johnson, W. Chen, M.W. Wong, C. Gonzalez and J.A. Pople, Gaussian 03 (Revision B.02), Gaussian, Inc., Pittsburgh, PA, 2003.
[38] (a) A.D. Becke, Phys. Rev. A 38 (1988) 3098;
(b) A.D. Becke, J. Chem. Phys. 98 (1993) 5648.
[39] (a) C. Lee, W. Yang, R.G. Parr, Phys. Rev. B 37 (1988) 785;
(b) J.P. Perdew, Y. Wang, Phys. Rev. B 45 (1992) 13244.
[40] (a) P.J. Hay, W.R. Wadt, J. Chem. Phys. 82 (1985) 270;
(b) W.R. Wadt, P.J. Hay, J. Chem. Phys. 82 (1985) 284;
(c) P.J. Hay, W.R. Wadt, J. Chem. Phys. 82 (1985) 299.
[41] M.M. Kappes, Chem. Rev. 88 (1988) 369.
[42] P.J. Linstrom, W.G. Mallard (Eds.), NIST Chemistry WebBook, NIST Standard Reference Database Number 69, National Institute of Standards and Technology, Gaithersburg, MD, 20899, http://webbook.nist.gov.
[43] F.A. Cotton, Advanced Inorganic Chemistry, 6th ed., John Wiley and Sons, Inc., New York, 1999.
[44] A.B.C. Patzer, C. Chang, E. Sedlmayr, D. Sülzle, Eur. Phys. J. 32 (2005) 329.